Genome-wide analysis of genetic pleiotropy and causal genes across three age-related ocular disorders

Xueming Yao, [1] Hongxi Yang, [2,a] Han Han, [1] Xuejing Kou, [1] Yuhan Jiang, [3] Menghan Luo, [3] Yao Zhou, [3] Jianhua Wang, [3] Xutong Fan, [3] Xiaohong Wang, [2,*] Mulin Jun Li, [2,3,*] Hua Yan[1,*]

[1] Department of Ophthalmology, Tianjin Medical University General Hospital, Tianjin, 300052, China.

[2] Department of Pharmacology, Tianjin Key Laboratory of Inflammation Biology, School of Basic Medical Sciences, Tianjin Medical University, Tianjin, 300070, China.

[3] Department of Bioinformatics, The Province and Ministry Co-sponsored Collaborative Innovation Center for Medical Epigenetics, School of Basic Medical Sciences, Tianjin Medical University, Tianjin, 300070, China.

[*]Correspondence: xiaohongwang@tmu.edu.cn (X.W.), mulin@tmu.edu.cn (M.J.L.), zyyyanhua@tmu.edu.cn (H.Y.)

[a] X.Y. and H.Y. contributed equally.

Abstract

Age-related macular disorder (AMD), cataract, and glaucoma are leading causes of blindness worldwide. Previous genome-wide association studies (GWASs) have revealed a variety of susceptible loci associated with age-related ocular disorders, yet the genetic pleiotropy and causal genes among these diseases remain poorly understood. By leveraging large-scale genetic and observational data from ocular disease GWASs and UK Biobank (UKBB), we found significant pairwise genetic correlations and epidemiological associations for these ocular disorders. Cross-disease meta-analysis uncovered ten pleiotropic loci, four of which were replicated in an additional cohort. Integration of variants in pleiotropic loci and multiple single-cell omics data identified that Müller cells and astrocytes were likely causal cell types underlying ocular comorbidity. In addition, we comprehensively integrated eye-specific gene expression quantitative loci (eQTLs), epigenomic profiling, and 3D genome data to prioritize causal pleiotropic genes. We found that pleiotropic genes were essential in nerve development and eye pigmentation, and targetable by existing drugs for the treatment of single ocular disorder. These findings will not only facilitate the mechanistic research of ocular comorbidities but also benefit the therapeutic optimization of age-related ocular diseases.

Introduction

Age-related ocular diseases, such as age-related macular degeneration (AMD), cataract, and glaucoma, are among the leading causes of irreversible blindness and vision impairment in adults aged ≥ 50 years worldwide [1]. Previous cross-sectional and case-control studies have reported that cataract and glaucoma commonly co-exist and prevalent glaucoma is associated with neovascular AMD [2; 3]. A clinical study also showed that over 20% of eye samples from the patients listed for cataract surgery have evidence of AMD according to optical coherence tomography imaging [4]. The findings motivate the exploration of the extent and causal factors for potential comorbidity among these age-related ocular diseases.

Recent genome-wide association studies (GWASs) have identified hundreds of genetic signals that contribute to the complex pathogenesis of AMD [5; 6], cataract,[7] and glaucoma [8-10]. These and other genetic studies also suggest a high heritability in susceptibility of AMD (~50%) [11], cataract (35-58%) [12; 13], and glaucoma (35-65%) [14; 15]. Nevertheless, the shared genetic architecture among these age-related ocular diseases is largely unknown. A study investigated the genetic pleiotropy among AMD and several eye-related diseases/traits, and found that patients with AMD demonstrate a genetically reduced risk to develop open-angle glaucoma [16], which is inconsistent with other findings [17; 18]. Moreover, no genetic pleiotropy research has been conducted between cataract and other ocular diseases so far. Given the conflicting results and scant knowledge regarding the shared genetic architecture of these age-related ocular disorders, more systematic investigation based on larger and complementary cohorts is needed.

While different levels of genetic correlations or pleiotropic loci can be faithfully estimated among ocular diseases/traits, the pleiotropic genes and causal variants have not been rigorously examined. This is an important issue to clarify, as the shared biological basis of ocular disorders could represent potential efficient intervention targets for the prevention and treatment of ocular comorbidities. Emerging tissue/cell type-specific epigenomic profiles, single-cell omics atlas as well as molecular phenotype quantitative trait loci (QTLs) mapping on certain ocular diseases revealed many causal variants and genes underlying cell type specificity of disease etiology [19-23]. Thus, integrating large-scale multi-omics and QTL data from eyes with disease pleiotropy information would provide a promising strategy to decipher the genetic causality of ocular comorbidities, especially for the majority of causal variants in the non-coding genomic regions.

Here, by leveraging large-scale genetic and observational data from public GWASs and UK Biobank (UKBB), we systematically investigated the genetic sharing patterns and epidemiological associations of three age-related ocular diseases including AMD, cataract, and glaucoma. We found extensive genetic pleiotropy and pairwise connections among these three diseases and identified ten pleiotropic loci across the genome. To better understand the mechanism underlying these pleiotropic loci, the integration of eye-specific gene expression (eQTLs), epigenomic profiling, and 3D genome data were conducted to probe causal pleiotropic genes. Finally, drug repurposing was conducted by utilizing molecular networks for potential treatment or prevention of ocular comorbidities.

Material and methods

GWAS summary statistics collection

Full GWAS summary statistics of European ancestry on AMD, cataract, and glaucoma with the largest sample size were obtained after searching eight databases (GWAS Catalog [24], UKBB [25], GeneATLAS [26], GWAS Atlas [27], LD Hub [28], GRASP [29], PhenoScanner [30], and dbGaP [31]). GWAS summary statistics with available signed statistics (beta or odds ratio), effect alleles, and non-effect alleles were retained during the search. We also collected GWAS summary data from FinnGen for replication analysis [32]. More detailed information regarding the selected GWAS summary statistics for AMD, cataract, and glaucoma was shown in **Table S1**.

Estimation of genetic correlation

Using GWAS summary statistics derived from the above datasets with a sample size > 50,000 and the number of cases and controls > 10,000, we conducted LD Score regression (LDSC) [33] for these ocular diseases to estimate pairwise genetic correlations. SNPs were filtered to HapMap3 SNPs to avoid bias due to inconsistent imputation quality. SNPs with INFO ≤ 0.9, minor allele frequency ≤ 0.01, non-SNP variants, strand-ambiguous SNPs, and SNPs with duplicate IDs were removed. Pre-computed linkage disequilibrium (LD) scores and regression weights for European populations of the 1000 Genomes project were downloaded from the LDSC website (http://www.broadinstitute.org/~bulik/eur_ldscores/). We ensured that the LD score regression intercepts for AMD, cataract, and glaucoma were close to 1 during estimations. Moreover, genetic correlations between these diseases were also estimated using another tool SumHer from LDAK [34] under the recommended LDAK-Thin model. A tagging file computed using 2,000 white British individual genetic data files was downloaded from the LDAK website

(https://dougspeed.com/pre-computed-tagging-files/), and the cutoff was set to 0.01 to preclude large-effect loci that explain at least 1% of phenotypic variance.

Mendelian randomization

Mendelian randomization (MR) analysis between two traits was performed to determine whether genetic correlations were due to a causal link or confounding factors using the R package TwoSampleMR [35] which encompasses five MR methods (MR Egger, Weighted median, Inverse variance weighted, Simple mode, Weighted mode). The instruments for each exposure trait were significant SNPs (P-value $< 5 \times 10^{-8}$) after clumping, while the instruments for each outcome trait were all SNPs. Variants without SNP ID were annotated using the dbSNP [36] database; otherwise, SNPs were removed during subsequent analyses.

Epidemiological analyses based on UK Biobank (UKBB) cohort

The UKBB is a large-scale cohort that recruited half a million UK participants (aged 37–73 years) between 2006 and 2010, and was followed up to 2021. Among the 502,412 participants, we excluded those who were pregnant (n = 379), lost to follow-up (n = 1,298), and had a mismatch between self-reported sex and genetic sex (n = 371), or missing information concerning covariates at baseline (n = 58,637). Overall, 441,727 participants were included in the study. AMD (ICD10: H35.3; ICD9: 362.5), cataract (ICD10: H25-H28; ICD9: 366), and glaucoma (ICD10: H40.1, H40.8, H40.9; ICD9: 365.1, 365.9) were ascertained based on information from self-reports, primary care records, hospital admissions, and death records. Multivariate Cox regression with separate models for incident AMD, cataract, and glaucoma was used to evaluate pairwise

associations among them. In subsequent analyses, multi-state models were used to examine the role of one of the three ocular diseases in the transition between the start of follow-up and the other two disorders. In all models, we adjusted for sex, age, ethnicity, Townsend deprivation index, education level, smoking status, drinking status, physical activity, screen time-based sedentary behavior, diabetes, and other eye problems. This research was conducted using the UKBB resource under application number 83974.

Determination of pleiotropic regions

We performed pleiotropic region analysis using gwas-pw [37], a tool for jointly analyzing pairs of GWAS traits. Overlapping SNPs of both traits were split into multiple blocks based on the bed files available at https://bitbucket.org/nygcresearch/ldetect-data. Separately, gwas-pw reckoned the posterior probability of the four models that the pleiotropic region 1) only associated with phenotype 1, 2) only associated with phenotype 2, 3) associated with both phenotypes, and 4) associated with both phenotypes independently.

Identification of pleiotropic loci

To identify pleiotropic variants and characterize pleiotropy at single-variant level, cross-trait meta-analyses were carried out with GWAS summary statistics of three ocular diseases using three different approaches: 1) ASSET [38], 2) METAL [39], and 3) pleioFDR [40]. ASSET explored all possible subsets of traits and evaluated a fixed-effect meta-analysis for each subset. The default scheme was selected when executing METAL with the correction of sample overlap. pleioFDR leveraged overlapping SNP associations of related phenotypes to identify genetic pleiotropic loci.

All significant SNPs involving two or more traits were retained for the following analysis. Once classified, we conducted variant clumping through PLINK [41] and merged the pleiotropic loci if they physically overlapped (±250kb). The summary statistics of these diseases were standardized using a downloaded reference derived from genome files for 22 autosomes of filtered the 1000 Genomes project [42] European ancestry samples.

Causal cell type estimation

We applied MAGMA [43] to evaluate whether specific ocular cell types showed significant heritability enrichment for traits based on ASSET one-sided summary statistics. MAGMA also requires gene average expression level across cell types derived from single-cell RNA sequencing (scRNA-seq) and single-cell multi-omics sequencing data of anterior chamber angle or retina/choroid [20; 21; 23; 44-46] (**Table S2**). We additionally downloaded the raw data and determined the average expression values per cell type for each dataset using Cell Ranger [47] and the R package Seurat [48] unless the information was available. Cell types were assigned with the gene marker mentioned in the original publications, and the same cell types were manually renamed to maintain concordance with different scRNA-seq data. Gene names were transferred to Entrez gene IDs using the R package biomaRt [49]. We appointed the direction of testing to "greater" and selected the condition-hide modifier for cell-type trait association analysis. We then leveraged the open chromatin peaks of retinal cell types from single-cell multiome to estimate LD scores for LDSC and conducted an additional cell-type trait association analysis.

Causal SNP identification at pleiotropic loci

Colocalization analysis between two-eye eQTL data [19; 50] and ASSET one-sided GWAS data was conducted using the R package COLOC [51]. We selected SNPs with an H4 posterior probability > 0.75, GWAS P-value < 1×10^{-6}, and eQTL P-value < 0.05 as pleiotropic loci. By utilizing three sets of retina sample Assay of Transposase Accessible Chromatin sequencing (ATAC-seq) and H3K27ac Chromatin immunoprecipitation followed by sequencing (ChIP-seq) data [52], genomic enhancer regions of the retina were predicted using the Activity-by-Contact (ABC) model [53] with default threshold settings. Next, we profiled the causal SNPs through fine-mapping analysis of pleiotropic loci identified by the above three meta-analysis methods. The one-sided ASSET meta-analysis results of pleiotropic SNPs located in the ± 1 Mb region of lead SNPs were imported into PolyFun [54] for fine-mapping with an embedded statistical method termed Susie [55], and 95% credible sets were revealed, assuming one causal SNP per locus. SNPs were included in the credible sets until the sum of the posterior probabilities was > 0.95.

Pleiotropic causal gene prioritization

The causal genes in a pleiotropic locus were confined to the following rules: 1) Does the locus contain eye eQTL SNPs? If yes, eQTL harboring genes (eGenes) were selected. 2) Is the locus located in the open chromatin peaks from retina H3K27ac HiChIP data [23]? If yes, causal genes were anchor-targeted genes. 3) Does the locus have a genomic region overlapping with the ABC model enhancer regions or a cell type-specific peak? If so, the causal genes were enhancer target genes or peak-inclusive genes. 4) If the pleiotropic locus contained none of the eQTL SNPs or was not mapped within any enhancer regions or peaks, the nearest gene with the highest COLOC posterior probability was identified as a causal gene. Moreover, gene ontology (GO) pathway

enrichment analysis of causal genes with no more than 10 interactors was conducted in STRING [56] to shed light on pathogenic biological processes, and gene-phenotype association analysis was conducted using Enrichr [57].

Drug repurposing analysis

We curated approved drugs targeted at pleiotropic causal genes and target genes of such drugs for AMD, cataract, and glaucoma from Drugbank [58] and DGIdb [59] to verify whether the risk genes were identical to the drug target genes. Protein-protein interaction (PPI) network information was obtained from STRING and depicted using Cytoscape [60] to evaluate potential relationships between pleiotropic causal genes and drug target genes.

Results

Genetic sharing among AMD, cataract, and glaucoma

To delineate the shared genetic architecture among the three age-related ocular disorders, we first collected full GWAS summary statistics of AMD, cataract, and glaucoma from the latest public resources, incorporating three AMD GWASs, three cataract GWASs and two glaucoma GWASs, and most of them had sample size over 100,000 individuals (**Table S1**). Considering the signal overlaps of the three largest ocular GWAS summary statistics (**Figure S1A**), genetic correlations were measured using LDSC [33] and SumHer LDAK-Thin [34] models. Following careful quality control, we observed moderate and concordant genome-wide genetic correlations among these traits (**Figure 1A, 1B, Figure S1B**), in which glaucoma-cataract and AMD-cataract showed positive genetic correlations, while AMD-glaucoma exhibited negative genetic correlations. This

is consistent with a previous study wherein the negative genetic correlation between AMD and glaucoma was reported [16]. In addition, multiple bidirectional MR methods were applied to each pair of diseases to assess whether shared genetic components were coherent with true pleiotropy or mediated pleiotropy. Presuming that consistent results in three of the five MR methods indicate a strong causal effect between the two traits, there was no or weak evidence for potentially causal relationships among AMD, cataract, and glaucoma (**Figure S2**).

Epidemiological associations among AMD, cataract, and glaucoma

To test whether the pattern of genetic sharing for the three age-related ocular disorders is supported by epidemiological associations, we leveraged 441,727 selected participants from the UKBB with rich information regarding self-reports, primary care records, hospital admissions, and death records. In the UKBB cohort, at the end of follow-up, 36,5471 (82.74%) participants had no AMD, cataract, or glaucoma; 5,611 (1.27 %) had AMD alone; 48,639 (11.01%) had cataract alone; 7,431 (1.68%) had glaucoma alone; 8,251 (1.87%) had both AMD and cataract; 1,329 (0.30%) had both AMD and glaucoma; 7,015 (1.59%) had both cataract and glaucoma; and 1,010 (0.23%) had AMD, cataract, and glaucoma. Hazard ratios (HRs) estimated by Cox regression were significantly larger than 1 (P-value < 0.001), which indicated positive correlations among these traits (**Figure 1A, Figure S3**). These results showed significant pairwise associations between AMD, cataract, and glaucoma. Similar results were observed in further analyses using multi-state models which also uncovered positive correlations between cataract and other diseases as genetic correlation analysis showed. The correlation between AMD and glaucoma was inconsistent with our genetic correlation results which may due to environmental effects or inadequate power.

Additionally, multi-state models distinguished the roles of one of the three prevalent ocular diseases in the temporal trajectories of the other two. Prevalent glaucoma was inversely associated with AMD after cataract with HR of 0.74 (95% CI: 0.64-0.86), but not with cataract after AMD (**Figure 1C**). Multi-state analyses also showed that the associations of prevalent cataracts with the transition from the start of follow-up to subsequent AMD or subsequent glaucoma were stronger than those with the transition from AMD to glaucoma or from glaucoma to AMD (**Figure 1D**). Accounting for prevalent AMD in transitions of cataract and glaucoma, there was no evidence of stronger associations between prevalent AMD and transitions to cataract after having had glaucoma, or glaucoma after having had cataract (**Figure 1E**). Taken together, these new findings based on genetic evidence and epidemiological associations suggested a latent correlation among age-related ocular traits.

Cross-disorder meta-analysis reveals ten pleiotropic loci

Considering the indication for genetic relationships between AMD-cataract, AMD-glaucoma, and cataract-glaucoma, 11 likely pleiotropic regions (posterior probability associated with two phenotypes > 0.6) were identified in the disease pairs using gwas-pw [37], one of which (chr9:20464018-2220526) turned out to be significant of two disease pairs (**Figure 1F, Table S3**). Next, we leveraged the largest collected GWAS summary statistics for AMD, cataract, and glaucoma containing 257,718 cases and 560,421 controls of European ancestry in total (AMD: 14,034 cases and 91,214 controls, cataract: 11,306 cases and 349,888 controls, glaucoma: 232,378 cases and 119,319 controls), and conducted cross-trait meta-analyses using three complementary methods including ASSET [38], METAL [39] and pleioFDR [40]. Only those SNPs that surpassed

genome-wide significance (P-value < 5×10^{-8}) and had influences on at least two traits were reserved. For ASSET, two patterns were supported, and both were performed such that the one-sided ASSET meta-analysis maximized the standard fixed-effect meta-analysis test statistics over all possible subsets and guaranteed the identification of pleiotropic loci that have associations in the same direction, while the two-sided ASSET meta-analysis was performed in two directions automatically. Accordingly, we identified 5, 10, 15, and 7 pleiotropic loci using METAL, one-sided ASSET, two-sided ASSET, and pleioFDR, respectively, under the condition that the genomic inflation factor did not considerably deviate from one (**Figure 2A, Figure S4, Figure S5**).

By guaranteeing that the lead SNPs were slightly significant in all primary GWAS summary statistics, ten loci were conservatively prioritized as candidate pleiotropic loci for which the one-sided ASSET results overlapped with the other three approaches (**Table 1**). Among these pleiotropic loci, most signals were significantly associated with glaucoma, and were even stronger after meta-analysis although they were weaker in other diseases. Notably, four novel loci (lead SNPs: rs3766916, rs17421627, rs11018564, rs146447071) became significant as the sample size increased. Besides, we found that four candidate pleiotropic loci intersected the aforementioned pleiotropic regions identified by gwas-pw (chr5:87390784-88891173, chr9:20464018-2220526, chr11:87430571-89208854, chr15:110336875-113261782) (**Table 1, Figure 1F**), which rendered our results convincing. Furthermore, we collected additional GWAS datasets of AMD, cataract, and glaucoma from FinnGen project [32] and conducted a meta-analysis with ASSET, four loci (lead SNPs: rs12670840, rs944801, rs1619882, and rs1129038) were replicated if the P-value of any

SNPs in the same loci was smaller than 1×10^{-5} in one-sided ASSET or two-sided ASSET results.

Single-cell multi-omics data integration identifies likely causal cell types of ocular comorbidity

To understand the causal disease mechanisms underlying these pleiotropic loci, we investigated which cell types are essential during the development of ocular comorbidity. We obtained six scRNA-seq datasets and a single-cell multiome dataset derived from 33 human eyes **(Table S2)** and performed cell-type trait association analysis to explore the most likely causal cell types whose gene or epigenomic signatures correlate with genetic pleiotropy. In total, more than 40 cell types across the anterior chamber angle and retina/choroid were used in our study. Consequently, Müller cells and astrocytes were concordantly estimated to be two causal cell types of ocular disease susceptibility using both MAGMA and LDSC (**Figure 2B, Figure S6, Table S4, Table S5**), suggesting that the two cell types could play a critical role in modulating ocular comorbidity. In addition, vascular endothelium and fibroblasts also displayed significant results in two or more MAGMA analyses (FDR < 0.05), which is consistent with previous study [20].

Functional prioritization of causal pleiotropic variants and their target genes

To identify the causal genes acting on genetic pleiotropy across the three age-related ocular disorders,

we first leveraged PolyFun [54] to fine-map the ten pleiotropic loci and identified causal variants in the 95% credible sets. We conducted colocalization analysis involving the ten pleiotropic loci

based on two retinal *cis*-eQTL datasets [19; 50], yielding a credible variant rs3766916 colocalizing at several eGenes, including *TRIM46* and *GON4L* (**Figure 2C, Figure S7, Table S6**). *TRIM46* encodes a protein of the tripartite motif family that controls neuronal polarity and high-glucose-induced ferroptosis in human retinal capillary endothelial cells [61], which suggests a potential causal role for retina-associated ocular traits.

Second, we collected retina H3K27ac HiChIP loops [23] to annotate all credible variants with spatially proximal genes. We found that three credible variants supported by HiChIP loops linked to different genes, and they were located in the eye enhancer regions or Müller cell/astrocyte open chromatin peaks according to single-cell multiome profiles. Notably, we found the SNP rs4845712 in high LD with rs3766916 (r^2 = 0.95 in European) may be more likely to be the causal SNP at the corresponding pleiotropic locus. rs4845712 in the intron of *EFNA4* gene received the highest posterior probability of fine-mapping analysis and overlapped with a retina H3K27ac HiChIP loop (**Figure 2D**). rs4845712 host gene *EFNA4* has been reported to inhibit axonal regeneration and regulate axon guidance in the optic nerve [62; 63], and its HiChIP target gene *CKS1B* encodes a protein that binds to the catalytic subunit of cyclin-dependent kinases, and proliferation and migration of retinoblastoma cells can be inhibited by suppressing the expression of *CKS1B* [64]. Another top credible SNP rs351973, close to *PTBP1* promoter region, can interact with the genomic region containing *KISS1R*, *R3HDM4*, and *ARID3A* genes (**Figure 3A**). Among these genes, knockdown of *Ptbp1* in mice effectively induces the conversion of Müller glia into retinal ganglion cells (RGCs), resulting in alleviation of disease symptoms pertinent to RGC loss [65].

Additionally, we applied ABC model [53] on ATAC-seq and H3K27ac ChIP-seq data from three retinal samples to predict enhancer-promoter interactions (**Table S7**). Based on the predicted interactions, target genes were achieved for an additional credible variant rs10898526. The SNP rs10898526 located at a pleiotropic locus prioritized by three meta-analysis methods and obtained Müller cell/astrocyte-specific open chromatin signatures. Target gene analysis based on ABC model suggested rs10898526 could interact with *ME3* gene promoter (**Figure 3B**). We found *ME3* was documented to involve in the oxidative decarboxylation of malate to pyruvate and associated with macular thickness [66]. Finally, for other credible variants without evidence of active chromatin marks or chromosome interactions, we annotated the nearest gene as the target gene for the top credible variant at the pleiotropic locus. The annotated and prioritized causal variants and their genes were shown in **Table S8**.

Shared biological pathways and drug repurposing opportunities

To assess the pleiotropic causal genes that affect biological pathways relevant to ocular diseases and explore the potential role of candidate genes in drug repurposing, we conducted several functional investigations. GO pathway analysis was first conducted in three orthogonal ontologies to explore the biological mechanisms of causal genes on ocular comorbidity. We detected 47 significant (FDR < 0.05) pathways, including the regulation of nerve development (GO:0021675, GO:0007409, and GO:0048666) (**Figure 4A, 4B, Table S9**). Multiple protein modification pathways were also enriched, such as regulation of the protein modification process (GO:0031399), protein phosphorylation (GO:0006468), and histone h3 acetylation (GO:0043966). In addition, *EFNA3*, *EFNA4*, and *SHC1* were hub genes in the PPI network of causal genes

(**Figure 4B**). We conducted gene-phenotype relationship analysis and revealed causal gene set was enriched for skin/hair/eye pigmentation (q-value = 0.0236) and eye color (q-value = 0.0008). We then linked genes to licensed drugs and found aspirin and zopiclone targeted the causal genes *ME3* and *GABRA5* separately. By searching the approved drugs and drug targets for AMD, cataract, and glaucoma in Drugbank [58] and DGIdb [59], we identified 88 drug targets for the ocular diseases and found 12 (40%) of the 30 causal genes interacting with these drug targets. Noteworthily, *EFNA4*, a gene identified as being involved in neuronal development in previous pathway analysis, interacted with aflibercept-targeted gene *VEGFA* and pilocarpine-targeted gene *NTRK1* in the PPI network of AMD and glaucoma (**Figure 4C, Figure 4D**), indicating the drug repurposing opportunities for the treatment of ocular comorbidity.

Discussion

In our study, we comprehensively investigated genetic sharing and epidemiological associations for three age-related ocular disorders. We confirmed the significant relationships among AMD, cataract, and glaucoma using a large-scale prospective observational study, genetic correlation analysis, and MR, followed by pleiotropic region analysis to explore regional pleiotropy. Ten significant pleiotropic loci of AMD, cataract, and glaucoma were identified using complementary meta-analyses, four of which achieved a marginally significant threshold in replication meta-analysis. In addition, we identified Müller cells and astrocytes as disease-associated cell types by single-cell multi-omics analysis. By incorporating statistical fine-mapping, retinal eQTL colocalization, and 3D genome loop data, we systematically prioritized causal target genes for pleiotropic variants. The interrogation of network biology was also implemented to identify

disease genes-associated molecules and pathways for potential drug repositioning of ocular disorders.

To our knowledge, no previous study has investigated the genetic and non-genetic associations among AMD, cataract, and glaucoma. Several observational, clinical, and genetic evidence strongly suggest a shared biological basis or similar pathophysiological mechanisms among these age-related ocular disorders [2-4; 16]. In this study, both epidemiological evidence based on large-scale UKBB data and genetic evidence based on several largest GWASs data supported pairwise tight associations between AMD, cataract, and glaucoma at different levels. The mechanisms behind our findings will shed light on the in-depth investigation of gene-environment interactions and comorbidity mechanisms across AMD, cataract, and glaucoma, which could also initiate further ocular disease comorbidity studies and emphasize the importance of comprehensive diagnosis and disease prevention in clinical practice.

By cross-disease meta-analysis at both variant and locus levels, we successfully identified ten pleiotropic loci. Nevertheless, understanding disease-causal cell types is of great value for the investigation of the precise mechanism between these loci-influenced genes and disease pathogenesis. We identified Müller cells and astrocytes as potential casual cell types for ocular comorbidity using two algorithms. A study claimed that Müller cells play a role in regulating serine biosynthesis, a critical part of the macular defense against oxidative stress, and their dysregulation may cause macular lesions [67]. Furthermore, Müller cells and astrocytes have multiple functions symbiotically associated with RGCs, such as glutamate clearance, neurotrophic

factor release, and neurotransmitter recycling [68], and the abnormality of RGCs will cause the impairment of visual acuity. Another study reported that the loss of astrocytes, together with retinal ischemia that occurs in AMD macula, could induce the death of RGCs owing to the oxidative damage [69]. Despite insufficient evidence in our study, a connection between macular vascular endothelium and these ocular diseases has been widely discussed [44; 70-73]. As a matrix cell type, fibroblasts can be activated by matricellular proteins, resulting in abnormal fibrotic processes in the extracellular matrix and subsequent elevated intraocular pressure [74]. In addition, fibroblasts may be recruited to neovascular lesions and differentiate into myofibroblasts, a key cell type in macular fibrosis secondary to neovascular AMD [75].

Leveraging pleiotropic genes we found, we nominated several ocular disease-related pathways like the regulation of nerve development. The optic nerve is made up of RGC axons and transmits visual signals from photoreceptor cells to the brain. Diminution of vision will occur once the transitions were hindered. Glaucoma is a neurodegenerative disorder manifesting selective, progressive, and irreversible degeneration of the optic nerve, and optic nerve regeneration in glaucoma treatment was wildly studied [76-78]. The photoreceptor synapses across retinas of patients with AMD retract into the outer nuclear layer which evokes the subsequent outgrowth and reformation of synaptic contacts [79]. Besides, optic nerve edema was found weeks to months after cataract extraction [80]. By conducting gene-phenotype relationship analysis, pleiotropic genes were related to eye color, which suggested the relevance to these age-related ocular diseases. Darker iris color is pertinent with increased risks of cataract and intraocular pressure and mitigated risks of AMD, uveal melanoma, and pigmentary glaucoma [14; 81-84].

There are a few shortcomings in these analyses. First, the relationship between AMD and glaucoma was not consistent between genetic correlation analysis and epidemiological evidence which may be due to environmental impact factors. More studies should be conducted to clarify the relationship between AMD and glaucoma. Second, the number of glaucoma cases was much larger than those for the other two diseases, and some controls may inevitably overlap in glaucoma and cataract, which may affect the power of signals and cause systemic errors and wrongly preferential shared effect in meta-analysis. Third, in the present study, we found several cell types related to these traits, however, based on limited public annotation data, tissue-level annotation profiles were leveraged rather than cell type-specific data to identify truly causal genes. Thus, genetic information regarding the eye needs to be interpreted more precisely and accurately. Fourth, our fine-mapping only yielded credible sets of variants under the assumption of one causal variant; therefore, the prioritized causal genes may be underestimated. In addition, although we found several signs connecting certain drug targets and causal pleiotropic genes, whether these drugs are beneficial or harmful to the phenotype is still unknown. Further experiments concerning drug discovery and repurposing need to be conducted in the future.

Declaration of interests

The authors declare no conflict of interest.

Acknowledgments

This study was supported by the National Natural Science Foundation of China (Grant Numbers

82020108007, 81830026, 32070675) and the Beijing-Tianjin-Hebei Special Project [Grant Number 19JCZDJC64300(Z), 20JCZXJC00180].

Author contributions

H.Y. and M.J.L. conceived of the project. X.Y., H.Y., and Y.J.performed the analyses. H.H., X.K., and M.L. contributed to the data collection and processing. Y.Z., J.W., and X.F. contributed to manuscript polishing and provided analysis suggestions. X.Y., M.J.L., and H.Y. wrote the manuscript. The authors read and approved the final submission.

Data and code availability

The published article includes all datasets analyzed during this study.

Reference

1. (2021). Trends in prevalence of blindness and distance and near vision impairment over 30 years: an analysis for the Global Burden of Disease Study. The Lancet Global health 9, e130-e143.

2. Vinod, K., Gedde, S.J., Feuer, W.J., Panarelli, J.F., Chang, T.C., Chen, P.P., and Parrish, R.K., 2nd. (2017). Practice Preferences for Glaucoma Surgery: A Survey of the American Glaucoma Society. Journal of glaucoma 26, 687-693.

3. Hu, C.C., Ho, J.D., Lin, H.C., and Kao, L.T. (2017). Association between open-angle glaucoma and neovascular age-related macular degeneration: a case-control study. Eye (London, England) 31, 872-877.

4. Weill, Y., Hanhart, J., Zadok, D., Smadja, D., Gelman, E., and Abulafia, A. (2021). Patient management modifications in cataract surgery candidates following incorporation of routine preoperative macular optical coherence tomography. J Cataract Refract Surg 47, 78-82.

5. Fritsche, L.G., Igl, W., Bailey, J.N., Grassmann, F., Sengupta, S., Bragg-Gresham, J.L., Burdon, K.P., Hebbring, S.J., Wen, C., Gorski, M., et al. (2016). A large genome-wide association study of age-related macular degeneration highlights contributions of rare and common variants. Nat Genet 48, 134-143.

6. Winkler, T.W., Grassmann, F., Brandl, C., Kiel, C., Gunther, F., Strunz, T., Weidner, L., Zimmermann, M.E., Korb, C.A., Poplawski, A., et al. (2020). Genome-wide association meta-analysis for early age-related macular degeneration highlights novel loci and insights for advanced disease. BMC Med Genomics 13, 120.

463 7. Choquet, H., Melles, R.B., Anand, D., Yin, J., Cuellar-Partida, G., Wang, W., andMe
464 Research, T., Hoffmann, T.J., Nair, K.S., Hysi, P.G., et al. (2021). A large multiethnic
465 GWAS meta-analysis of cataract identifies new risk loci and sex-specific effects. Nat
466 Commun 12, 3595.
467 8. Khawaja, A.P., Cooke Bailey, J.N., Wareham, N.J., Scott, R.A., Simcoe, M., Igo, R.P., Jr.,
468 Song, Y.E., Wojciechowski, R., Cheng, C.Y., Khaw, P.T., et al. (2018). Genome-wide
469 analyses identify 68 new loci associated with intraocular pressure and improve risk
470 prediction for primary open-angle glaucoma. Nat Genet 50, 778-782.
471 9. Gharahkhani, P., Jorgenson, E., Hysi, P., Khawaja, A.P., Pendergrass, S., Han, X., Ong,
472 J.S., Hewitt, A.W., Segre, A.V., Rouhana, J.M., et al. (2021). Genome-wide
473 meta-analysis identifies 127 open-angle glaucoma loci with consistent effect across
474 ancestries. Nat Commun 12, 1258.
475 10. Mackey, D.A., and Hewitt, A.W. (2014). Genome-wide association study success in
476 ophthalmology. Curr Opin Ophthalmol 25, 386-393.
477 11. Seddon, J.M., Cote, J., Page, W.F., Aggen, S.H., and Neale, M.C. (2005). The US twin
478 study of age-related macular degeneration: relative roles of genetic and environmental
479 influences. Arch Ophthalmol 123, 321-327.
480 12. Hammond, C.J., Snieder, H., Spector, T.D., and Gilbert, C.E. (2000). Genetic and
481 environmental factors in age-related nuclear cataracts in monozygotic and dizygotic
482 twins. N Engl J Med 342, 1786-1790.
483 13. Yonova-Doing, E., Forkin, Z.A., Hysi, P.G., Williams, K.M., Spector, T.D., Gilbert, C.E., and
484 Hammond, C.J. (2016). Genetic and Dietary Factors Influencing the Progression of

485 Nuclear Cataract. Ophthalmology 123, 1237-1244.

486 14. Simcoe, M.J., Weisschuh, N., Wissinger, B., Hysi, P.G., and Hammond, C.J. (2020).
487 Genetic Heritability of Pigmentary Glaucoma and Associations With Other Eye
488 Phenotypes. JAMA ophthalmology 138, 294-299.

489 15. van Koolwijk, L.M., Despriet, D.D., van Duijn, C.M., Pardo Cortes, L.M., Vingerling, J.R.,
490 Aulchenko, Y.S., Oostra, B.A., Klaver, C.C., and Lemij, H.G. (2007). Genetic
491 contributions to glaucoma: heritability of intraocular pressure, retinal nerve fiber layer
492 thickness, and optic disc morphology. Investigative ophthalmology & visual science 48,
493 3669-3676.

494 16. Grassmann, F., Kiel, C., Zimmermann, M.E., Gorski, M., Grassmann, V., Stark, K.,
495 International, A.M.D.G.C., Heid, I.M., and Weber, B.H. (2017). Genetic pleiotropy
496 between age-related macular degeneration and 16 complex diseases and traits.
497 Genome Med 9, 29.

498 17. Cuellar-Partida, G., Craig, J.E., Burdon, K.P., Wang, J.J., Vote, B.J., Souzeau, E.,
499 McAllister, I.L., Isaacs, T., Lake, S., Mackey, D.A., et al. (2016). Assessment of
500 polygenic effects links primary open-angle glaucoma and age-related macular
501 degeneration. Scientific reports 6, 26885.

502 18. Xue, Z., Yuan, J., Chen, F., Yao, Y., Xing, S., Yu, X., Li, K., Wang, C., Bao, J., Qu, J., et al.
503 (2022). Genome-wide association meta-analysis of 88,250 individuals highlights
504 pleiotropic mechanisms of five ocular diseases in UK Biobank. EBioMedicine 82,
505 104161.

506 19. Ratnapriya, R., Sosina, O.A., Starostik, M.R., Kwicklis, M., Kapphahn, R.J., Fritsche, L.G.,

507 Walton, A., Arvanitis, M., Gieser, L., Pietraszkiewicz, A., et al. (2019). Retinal
508 transcriptome and eQTL analyses identify genes associated with age-related macular
509 degeneration. Nature genetics 51, 606-610.
510 20. Orozco, L.D., Chen, H.H., Cox, C., Katschke, K.J., Jr., Arceo, R., Espiritu, C., Caplazi, P.,
511 Nghiem, S.S., Chen, Y.J., Modrusan, Z., et al. (2020). Integration of eQTL and a
512 Single-Cell Atlas in the Human Eye Identifies Causal Genes for Age-Related Macular
513 Degeneration. Cell reports 30, 1246-1259.e1246.
514 21. Menon, M., Mohammadi, S., Davila-Velderrain, J., Goods, B.A., Cadwell, T.D., Xing, Y.,
515 Stemmer-Rachamimov, A., Shalek, A.K., Love, J.C., Kellis, M., et al. (2019).
516 Single-cell transcriptomic atlas of the human retina identifies cell types associated with
517 age-related macular degeneration. Nat Commun 10, 4902.
518 22. Wang, J., Zibetti, C., Shang, P., Sripathi, S.R., Zhang, P., Cano, M., Hoang, T., Xia, S., Ji,
519 H., Merbs, S.L., et al. (2018). ATAC-Seq analysis reveals a widespread decrease of
520 chromatin accessibility in age-related macular degeneration. Nature communications
521 9, 1364.
522 23. Wang, S.K., Nair, S., Li, R., Kraft, K., Pampari, A., Patel, A., Kang, J.B., Luong, C.,
523 Kundaje, A., and Chang, H.Y. (2022). Single-cell multiome of the human retina and
524 deep learning nominate causal variants in complex eye diseases. bioRxiv,
525 2022.2003.2009.483684.
526 24. Buniello, A., MacArthur, J.A.L., Cerezo, M., Harris, L.W., Hayhurst, J., Malangone, C.,
527 McMahon, A., Morales, J., Mountjoy, E., Sollis, E., et al. (2019). The NHGRI-EBI
528 GWAS Catalog of published genome-wide association studies, targeted arrays and

529 summary statistics 2019. Nucleic acids research 47, D1005-d1012.

530 25. Sudlow, C., Gallacher, J., Allen, N., Beral, V., Burton, P., Danesh, J., Downey, P., Elliott, P.,
531 Green, J., Landray, M., et al. (2015). UK biobank: an open access resource for
532 identifying the causes of a wide range of complex diseases of middle and old age.
533 PLoS medicine 12, e1001779.

534 26. Canela-Xandri, O., Rawlik, K., and Tenesa, A. (2018). An atlas of genetic associations in
535 UK Biobank. Nature genetics 50, 1593-1599.

536 27. Watanabe, K., Stringer, S., Frei, O., Umićević Mirkov, M., de Leeuw, C., Polderman, T.J.C.,
537 van der Sluis, S., Andreassen, O.A., Neale, B.M., and Posthuma, D. (2019). A global
538 overview of pleiotropy and genetic architecture in complex traits. Nature genetics 51,
539 1339-1348.

540 28. Zheng, J., Erzurumluoglu, A.M., Elsworth, B.L., Kemp, J.P., Howe, L., Haycock, P.C.,
541 Hemani, G., Tansey, K., Laurin, C., Pourcain, B.S., et al. (2017). LD Hub: a centralized
542 database and web interface to perform LD score regression that maximizes the
543 potential of summary level GWAS data for SNP heritability and genetic correlation
544 analysis. Bioinformatics (Oxford, England) 33, 272-279.

545 29. Leslie, R., O'Donnell, C.J., and Johnson, A.D. (2014). GRASP: analysis of
546 genotype-phenotype results from 1390 genome-wide association studies and
547 corresponding open access database. Bioinformatics (Oxford, England) 30, i185-194.

548 30. Kamat, M.A., Blackshaw, J.A., Young, R., Surendran, P., Burgess, S., Danesh, J.,
549 Butterworth, A.S., and Staley, J.R. (2019). PhenoScanner V2: an expanded tool for
550 searching human genotype-phenotype associations. Bioinformatics (Oxford, England)

551 35, 4851-4853.

552 31. Mailman, M.D., Feolo, M., Jin, Y., Kimura, M., Tryka, K., Bagoutdinov, R., Hao, L., Kiang,
553 A., Paschall, J., Phan, L., et al. (2007). The NCBI dbGaP database of genotypes and
554 phenotypes. Nature genetics 39, 1181-1186.

555 32. Kurki, M.I., Karjalainen, J., Palta, P., Sipilä, T.P., Kristiansson, K., Donner, K., Reeve, M.P.,
556 Laivuori, H., Aavikko, M., Kaunisto, M.A., et al. (2022). FinnGen: Unique genetic
557 insights from combining isolated population and national health register data. medRxiv,
558 2022.2003.2003.22271360.

559 33. Bulik-Sullivan, B., Finucane, H.K., Anttila, V., Gusev, A., Day, F.R., Loh, P.R., Duncan, L.,
560 Perry, J.R., Patterson, N., Robinson, E.B., et al. (2015). An atlas of genetic
561 correlations across human diseases and traits. Nature genetics 47, 1236-1241.

562 34. Zhang, Q., Privé, F., Vilhjálmsson, B., and Speed, D. (2021). Improved genetic prediction
563 of complex traits from individual-level data or summary statistics. Nature
564 communications 12, 4192.

565 35. Hemani, G., Zheng, J., Elsworth, B., Wade, K.H., Haberland, V., Baird, D., Laurin, C.,
566 Burgess, S., Bowden, J., Langdon, R., et al. (2018). The MR-Base platform supports
567 systematic causal inference across the human phenome. eLife 7.

568 36. Sherry, S.T., Ward, M.H., Kholodov, M., Baker, J., Phan, L., Smigielski, E.M., and Sirotkin,
569 K. (2001). dbSNP: the NCBI database of genetic variation. Nucleic acids research 29,
570 308-311.

571 37. Pickrell, J.K., Berisa, T., Liu, J.Z., Ségurel, L., Tung, J.Y., and Hinds, D.A. (2016).
572 Detection and interpretation of shared genetic influences on 42 human traits. Nature

573 genetics 48, 709-717.

574 38. Bhattacharjee, S., Rajaraman, P., Jacobs, K.B., Wheeler, W.A., Melin, B.S., Hartge, P.,
575 Yeager, M., Chung, C.C., Chanock, S.J., and Chatterjee, N. (2012). A subset-based
576 approach improves power and interpretation for the combined analysis of genetic
577 association studies of heterogeneous traits. American journal of human genetics 90,
578 821-835.

579 39. Willer, C.J., Li, Y., and Abecasis, G.R. (2010). METAL: fast and efficient meta-analysis of
580 genomewide association scans. Bioinformatics (Oxford, England) 26, 2190-2191.

581 40. Andreassen, O.A., Thompson, W.K., Schork, A.J., Ripke, S., Mattingsdal, M., Kelsoe, J.R.,
582 Kendler, K.S., O'Donovan, M.C., Rujescu, D., Werge, T., et al. (2013). Improved
583 detection of common variants associated with schizophrenia and bipolar disorder
584 using pleiotropy-informed conditional false discovery rate. PLoS genetics 9,
585 e1003455.

586 41. Purcell, S., Neale, B., Todd-Brown, K., Thomas, L., Ferreira, M.A., Bender, D., Maller, J.,
587 Sklar, P., de Bakker, P.I., Daly, M.J., et al. (2007). PLINK: a tool set for whole-genome
588 association and population-based linkage analyses. American journal of human
589 genetics 81, 559-575.

590 42. Auton, A., Brooks, L.D., Durbin, R.M., Garrison, E.P., Kang, H.M., Korbel, J.O., Marchini,
591 J.L., McCarthy, S., McVean, G.A., and Abecasis, G.R. (2015). A global reference for
592 human genetic variation. Nature 526, 68-74.

593 43. de Leeuw, C.A., Mooij, J.M., Heskes, T., and Posthuma, D. (2015). MAGMA: generalized
594 gene-set analysis of GWAS data. PLoS computational biology 11, e1004219.

595 44. Voigt, A.P., Mulfaul, K., Mullin, N.K., Flamme-Wiese, M.J., Giacalone, J.C., Stone, E.M.,
596 Tucker, B.A., Scheetz, T.E., and Mullins, R.F. (2019). Single-cell transcriptomics of
597 the human retinal pigment epithelium and choroid in health and macular degeneration.
598 Proceedings of the National Academy of Sciences of the United States of America 116,
599 24100-24107.
600 45. van Zyl, T., Yan, W., McAdams, A., Peng, Y.R., Shekhar, K., Regev, A., Juric, D., and
601 Sanes, J.R. (2020). Cell atlas of aqueous humor outflow pathways in eyes of humans
602 and four model species provides insight into glaucoma pathogenesis. Proceedings of
603 the National Academy of Sciences of the United States of America 117, 10339-10349.
604 46. Patel, G., Fury, W., Yang, H., Gomez-Caraballo, M., Bai, Y., Yang, T., Adler, C., Wei, Y., Ni,
605 M., Schmitt, H., et al. (2020). Molecular taxonomy of human ocular outflow tissues
606 defined by single-cell transcriptomics. Proceedings of the National Academy of
607 Sciences of the United States of America 117, 12856-12867.
608 47. Zheng, G.X., Terry, J.M., Belgrader, P., Ryvkin, P., Bent, Z.W., Wilson, R., Ziraldo, S.B.,
609 Wheeler, T.D., McDermott, G.P., Zhu, J., et al. (2017). Massively parallel digital
610 transcriptional profiling of single cells. Nature communications 8, 14049.
611 48. Hao, Y., Hao, S., Andersen-Nissen, E., Mauck, W.M., 3rd, Zheng, S., Butler, A., Lee, M.J.,
612 Wilk, A.J., Darby, C., Zager, M., et al. (2021). Integrated analysis of multimodal
613 single-cell data. Cell 184, 3573-3587.e3529.
614 49. Durinck, S., Spellman, P.T., Birney, E., and Huber, W. (2009). Mapping identifiers for the
615 integration of genomic datasets with the R/Bioconductor package biomaRt. Nature
616 protocols 4, 1184-1191.

617 50. Strunz, T., Kiel, C., Grassmann, F., Ratnapriya, R., Kwicklis, M., Karlstetter, M., Fauser, S.,
618 Arend, N., Swaroop, A., Langmann, T., et al. (2020). A mega-analysis of expression
619 quantitative trait loci in retinal tissue. PLoS genetics 16, e1008934.
620 51. Giambartolomei, C., Vukcevic, D., Schadt, E.E., Franke, L., Hingorani, A.D., Wallace, C.,
621 and Plagnol, V. (2014). Bayesian test for colocalisation between pairs of genetic
622 association studies using summary statistics. PLoS genetics 10, e1004383.
623 52. Cherry, T.J., Yang, M.G., Harmin, D.A., Tao, P., Timms, A.E., Bauwens, M., Allikmets, R.,
624 Jones, E.M., Chen, R., De Baere, E., et al. (2020). Mapping the cis-regulatory
625 architecture of the human retina reveals noncoding genetic variation in disease.
626 Proceedings of the National Academy of Sciences of the United States of America 117,
627 9001-9012.
628 53. Fulco, C.P., Nasser, J., Jones, T.R., Munson, G., Bergman, D.T., Subramanian, V.,
629 Grossman, S.R., Anyoha, R., Doughty, B.R., Patwardhan, T.A., et al. (2019).
630 Activity-by-contact model of enhancer-promoter regulation from thousands of CRISPR
631 perturbations. Nature genetics 51, 1664-1669.
632 54. Weissbrod, O., Hormozdiari, F., Benner, C., Cui, R., Ulirsch, J., Gazal, S., Schoech, A.P.,
633 van de Geijn, B., Reshef, Y., Márquez-Luna, C., et al. (2020). Functionally informed
634 fine-mapping and polygenic localization of complex trait heritability. Nature genetics
635 52, 1355-1363.
636 55. Wang, G., Sarkar, A., Carbonetto, P., and Stephens, M. (2020). A simple new approach to
637 variable selection in regression, with application to genetic fine mapping. Journal of
638 the Royal Statistical Society: Series B (Statistical Methodology) 82, 1273-1300.

639 56. Szklarczyk, D., Gable, A.L., Lyon, D., Junge, A., Wyder, S., Huerta-Cepas, J., Simonovic,
640 M., Doncheva, N.T., Morris, J.H., Bork, P., et al. (2019). STRING v11: protein-protein
641 association networks with increased coverage, supporting functional discovery in
642 genome-wide experimental datasets. Nucleic acids research 47, D607-d613.
643 57. Xie, Z., Bailey, A., Kuleshov, M.V., Clarke, D.J.B., Evangelista, J.E., Jenkins, S.L.,
644 Lachmann, A., Wojciechowicz, M.L., Kropiwnicki, E., Jagodnik, K.M., et al. (2021).
645 Gene Set Knowledge Discovery with Enrichr. Current protocols 1, e90.
646 58. Wishart, D.S., Knox, C., Guo, A.C., Shrivastava, S., Hassanali, M., Stothard, P., Chang, Z.,
647 and Woolsey, J. (2006). DrugBank: a comprehensive resource for in silico drug
648 discovery and exploration. Nucleic acids research 34, D668-672.
649 59. Freshour, S.L., Kiwala, S., Cotto, K.C., Coffman, A.C., McMichael, J.F., Song, J.J., Griffith,
650 M., Griffith, O.L., and Wagner, A.H. (2021). Integration of the Drug-Gene Interaction
651 Database (DGIdb 4.0) with open crowdsource efforts. Nucleic acids research 49,
652 D1144-d1151.
653 60. Shannon, P., Markiel, A., Ozier, O., Baliga, N.S., Wang, J.T., Ramage, D., Amin, N.,
654 Schwikowski, B., and Ideker, T. (2003). Cytoscape: a software environment for
655 integrated models of biomolecular interaction networks. Genome research 13,
656 2498-2504.
657 61. Zhang, J., Qiu, Q., Wang, H., Chen, C., and Luo, D. (2021). TRIM46 contributes to high
658 glucose-induced ferroptosis and cell growth inhibition in human retinal capillary
659 endothelial cells by facilitating GPX4 ubiquitination. Experimental cell research 407,
660 112800.

661 62. Goldshmit, Y., Galea, M.P., Wise, G., Bartlett, P.F., and Turnley, A.M. (2004). Axonal
662 regeneration and lack of astrocytic gliosis in EphA4-deficient mice. The Journal of
663 neuroscience : the official journal of the Society for Neuroscience 24, 10064-10073.
664 63. Kozulin, P., Natoli, R., O'Brien, K.M., Madigan, M.C., and Provis, J.M. (2009). Differential
665 expression of anti-angiogenic factors and guidance genes in the developing macula.
666 Molecular vision 15, 45-59.
667 64. Zeng, Z., Gao, Z.L., Zhang, Z.P., Jiang, H.B., Yang, C.Q., Yang, J., and Xia, X.B. (2019).
668 Downregulation of CKS1B restrains the proliferation, migration, invasion and
669 angiogenesis of retinoblastoma cells through the MEK/ERK signaling pathway.
670 International journal of molecular medicine 44, 103-114.
671 65. Zhou, H., Su, J., Hu, X., Zhou, C., Li, H., Chen, Z., Xiao, Q., Wang, B., Wu, W., Sun, Y., et
672 al. (2020). Glia-to-Neuron Conversion by CRISPR-CasRx Alleviates Symptoms of
673 Neurological Disease in Mice. Cell 181, 590-603.e516.
674 66. Francis, P.J. (2011). The influence of genetics on response to treatment with ranibizumab
675 (Lucentis) for age-related macular degeneration: the Lucentis Genotype Study (an
676 American Ophthalmological Society thesis). Transactions of the American
677 Ophthalmological Society 109, 115-156.
678 67. Zhang, T., Zhu, L., Madigan, M.C., Liu, W., Shen, W., Cherepanoff, S., Zhou, F., Zeng, S.,
679 Du, J., and Gillies, M.C. (2019). Human macular Müller cells rely more on serine
680 biosynthesis to combat oxidative stress than those from the periphery. eLife 8.
681 68. García-Bermúdez, M.Y., Freude, K.K., Mouhammad, Z.A., van Wijngaarden, P., Martin,
682 K.K., and Kolko, M. (2021). Glial Cells in Glaucoma: Friends, Foes, and Potential

683 Therapeutic Targets. Frontiers in neurology 12, 624983.

684 69. Ramírez, J.M., Ramírez, A.I., Salazar, J.J., de Hoz, R., and Triviño, A. (2001). Changes of
685 astrocytes in retinal ageing and age-related macular degeneration. Experimental eye
686 research 73, 601-615.

687 70. Fu, D.J., Keenan, T.D., Faes, L., Lim, E., Wagner, S.K., Moraes, G., Huemer, J., Kern, C.,
688 Patel, P.J., Balaskas, K., et al. (2021). Insights From Survival Analyses During 12
689 Years of Anti-Vascular Endothelial Growth Factor Therapy for Neovascular
690 Age-Related Macular Degeneration. JAMA ophthalmology 139, 57-67.

691 71. Klein, B.E., Klein, R., Lee, K.E., Knudtson, M.D., and Tsai, M.Y. (2006). Markers of
692 inflammation, vascular endothelial dysfunction, and age-related cataract. American
693 journal of ophthalmology 141, 116-122.

694 72. Bukhari, S.M., Kiu, K.Y., Thambiraja, R., Sulong, S., Rasool, A.H., and Liza-Sharmini, A.T.
695 (2016). Microvascular endothelial function and severity of primary open angle
696 glaucoma. Eye (London, England) 30, 1579-1587.

697 73. Su, W.W., Cheng, S.T., Ho, W.J., Tsay, P.K., Wu, S.C., and Chang, S.H. (2008).
698 Glaucoma is associated with peripheral vascular endothelial dysfunction.
699 Ophthalmology 115, 1173-1178.e1171.

700 74. Wallace, D.M., Murphy-Ullrich, J.E., Downs, J.C., and O'Brien, C.J. (2014). The role of
701 matricellular proteins in glaucoma. Matrix biology : journal of the International Society
702 for Matrix Biology 37, 174-182.

703 75. Little, K., Ma, J.H., Yang, N., Chen, M., and Xu, H. (2018). Myofibroblasts in macular
704 fibrosis secondary to neovascular age-related macular degeneration - the potential

705 sources and molecular cues for their recruitment and activation. EBioMedicine 38,
706 283-291.
707 76. Yuan, F., Wang, M., Jin, K., and Xiang, M. (2021). Advances in Regeneration of Retinal
708 Ganglion Cells and Optic Nerves. International journal of molecular sciences 22.
709 77. You, M., Rong, R., Zeng, Z., Xia, X., and Ji, D. (2021). Transneuronal Degeneration in the
710 Brain During Glaucoma. Frontiers in aging neuroscience 13, 643685.
711 78. Williams, P.R., Benowitz, L.I., Goldberg, J.L., and He, Z. (2020). Axon Regeneration in the
712 Mammalian Optic Nerve. Annual review of vision science 6, 195-213.
713 79. Sullivan, R.K., Woldemussie, E., and Pow, D.V. (2007). Dendritic and synaptic plasticity of
714 neurons in the human age-related macular degeneration retina. Investigative
715 ophthalmology & visual science 48, 2782-2791.
716 80. McCulley, T.J. (2012). Ischemic optic neuropathy and cataract extraction: What do I need
717 to know? Oman journal of ophthalmology 5, 141-143.
718 81. Sun, H.P., Lin, Y., and Pan, C.W. (2014). Iris color and associated pathological ocular
719 complications: a review of epidemiologic studies. International journal of
720 ophthalmology 7, 872-878.
721 82. Mitchell, R., Rochtchina, E., Lee, A., Wang, J.J., and Mitchell, P. (2003). Iris color and
722 intraocular pressure: the Blue Mountains Eye Study. American journal of
723 ophthalmology 135, 384-386.
724 83. McGowan, A., Silvestri, G., Moore, E., Silvestri, V., Patterson, C.C., Maxwell, A.P., and
725 McKay, G.J. (2014). Retinal vascular caliber, iris color, and age-related macular
726 degeneration in the Irish Nun Eye Study. Investigative ophthalmology & visual science

727 56, 382-387.

728 84. Frank, R.N., Puklin, J.E., Stock, C., and Canter, L.A. (2000). Race, iris color, and

729 age-related macular degeneration. Transactions of the American Ophthalmological

730 Society 98, 109-115; discussion 115-107.

731

732

Figure legends

Figure 1. Genetic pleiotropy of ocular disorders at the genomic level and regional level.

A. Epidemiological and genetic correlations between AMD, cataract, and glaucoma. Significant and strongest genetic correlations of disparate methods are shown. Red: hazard ratios estimated by Cox regression; blue: genetic correlations estimated by LDSC; yellow: genetic correlations estimated by LDAK. **B.** Genetic correlations of AMD, cataract, and glaucoma estimated by LDSC. The size and color of circles show the genetic correlations of disease pairs and the black stars indicate significant results and. **C.** Multi-state models for the role of glaucoma in transitions to other two diseases. **D.** Multi-state models for the role of cataract in transitions to other two diseases. **E.** Multi-state models for the role of AMD in transitions to other two diseases. **D.** Chromosome graphics showing the pleiotropic regions assessed by gwas-pw. A partial enlarged view shows the pleiotropic region resided in chromosome 9 which overlapped with one locus identified by meta-analysis. Different color dots represent the posterior probability of trait pairs (red: AMD-cataract; blue: AMD-glaucoma; green: cataract-glaucoma). The dashed line represents the predictive threshold of posterior probability > 0.6.

Figure 2. The pleiotropic loci of ocular phenotypes as well as trait-associated cell types.

A. Circular Manhattan plot of the meta-analysis results using one-sided ASSET. The orange triangles denote the lead SNPs of pleiotropic loci identified by three meta-analysis methods. The texts beside triangles show the nearest genes of these loci. The arcs in the outer layer represent chromosome positions and the number of SNPs in each position is depicted with different colors. Each dot in the inner layer represents a SNP and the red circle indicates the genome-wide significant threshold (P-value = 5×10^{-8}). **B.** The significance of various cell types from

MAGMA and LDSC in the cell-type trait association analysis. The significant cell types after Benjamini-Hochberg correction (FDR < 0.05) are highlighted. **C.** Locus-compare plots of lead SNP rs3766916 with macular eQTL gene TRIM46. Different colors of dots represent the linkage disequilibrium between the lead SNP (colored purple) and corresponding SNP. **D.** Locuszoom plots of one-sided ASSET associations and posterior probability of causality for variants around risk SNP rs4845712 which overlaps with *EFNA3* enhancer and retinal H3K27ac HiChIP data. The risk variant is uniquely highlighted with purple and all other SNPs are highlighted by their r^2. The overlapped open chromatin peaks of 13 retinal cell types are shown in the middle. Anchor regions of the retina are highlighted with an orange or blue rectangle and red arcs show the enhance-gene pairs predicted by Activity-by-Contact model. Genes in red and blue represent the sense and antisense directions, respectively. The dashed line indicated the interested SNP position.

Figure 3. Integration with retinal eQTLs, epigenomic, and 3D genome data for causal genes prioritization.

A. Locuszoom plots of one-sided ASSET associations and posterior probability of causality for variants around risk SNP rs351973 which reside in one of the HiChIP anchors. **B.** Locuszoom plots of one-sided ASSET associations and posterior probability of causality for variants around risk SNP rs10898526 which overlaps with *ME3* predicted enhancer. The risk variant is uniquely highlighted with purple and all other SNPs are highlighted by their r^2. The overlapped open chromatin peaks of 13 retinal cell types were shown in the middle. Anchor regions of the retina were highlighted with an orange or blue rectangle and red arcs show the enhance-gene pairs predicted by Activity-by-Contact model. Genes in red and blue represent the sense and antisense directions, respectively. The dashed line indicated the interested SNP position.

Figure 4. Functional enrichment of pleiotropic causal genes and drug repositioning for the treatment of ocular comorbidity.

A. Gene ontology pathway enrichment analysis of pleiotropic causal genes. The size and color of the circles indicated the number of causal genes and the significance in the corresponding pathway. **B.** Protein-protein interaction (PPI) network of causal genes. The red text with larger nodes indicated the pleiotropic gene in three diseases while the purple text indicated pleiotropic genes in two diseases. The thickness of the edges represents the strength of evidence. **C. & D.** PPI networks using disease-risk genes (red) and drug-targeted genes (purple and light gray). The nodes in light blue ellipses represent the lateral drug target genes.

Tables

Table 1. The ten pleiotropic loci identified by three meta-analysis approaches

Chr	SNP ID	Position	*P*-value	A1	A2	Diseases	Nearest gene(s)
1	rs3766916	155049402	3.03E-09	T	C	glaucoma, AMD, cataract	*EFNA3*
3	rs35050931	150058352	6.69E-11	T	A	glaucoma, cataract	*TSC22D2*
5	rs17421627	87847586	1.83E-08	T	G	glaucoma, AMD	*LINC00461*
6	rs13191376	45522139	1.66E-09	C	T	glaucoma, cataract	*RUNX2*
7	rs12670840	116125172	7.52E-21	C	T	glaucoma, AMD, cataract	*CAV2*
9	rs944801	22051670	8.00E-42	G	C	glaucoma, cataract	*CDKN2B-AS1*
11	rs1619882	86363742	2.73E-17	C	A	glaucoma, AMD, cataract	*ME3*
11	rs11018564	89035134	2.89E-08	T	C	glaucoma, cataract	*TYR*, *NOX4*
15	rs1129038	28356859	5.26E-13	C	T	glaucoma, AMD, cataract	*HERC2*
19	rs146447071	818751	5.40E-09	T	C	glaucoma, cataract	*LPPR3*

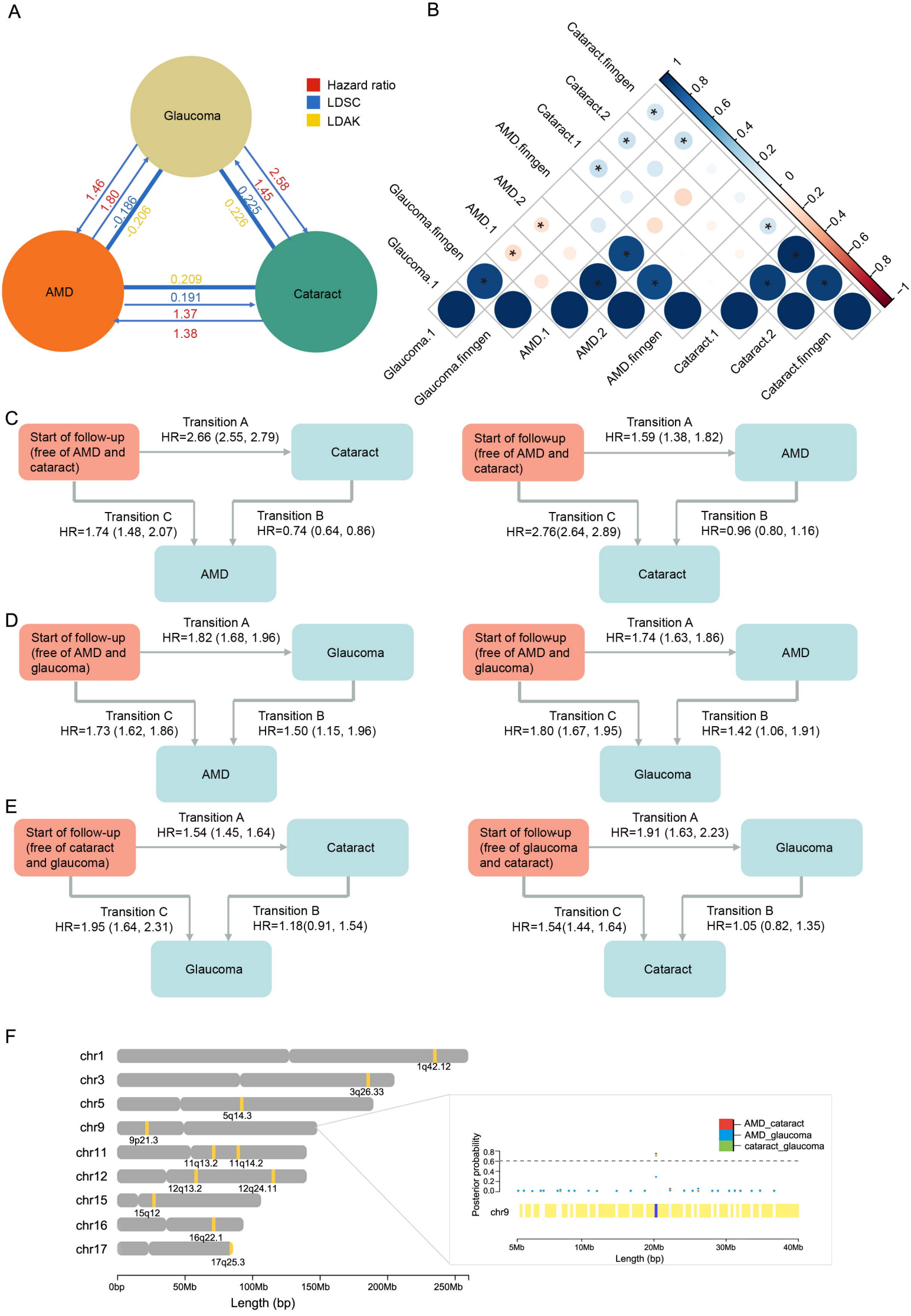
A
Glaucoma
AMD
Cataract
Hazard ratio
LDSC
LDAK
1.46
1.80
-0.186
-0.206
2.58
1.45
0.225
0.226
0.209
0.191
1.37
1.38
B
Cataract.finngen
Cataract.2
Cataract.1
AMD.finngen
AMD.2
AMD.1
Glaucoma.finngen
Glaucoma.1
1
0.8
0.6
0.4
0.2
0
-0.2
-0.4
-0.6
-0.8
-1
C
Start of follow-up (free of AMD and cataract)
Transition A HR=2.66 (2.55, 2.79)
Cataract
Transition C HR=1.74 (1.48, 2.07)
Transition B HR=0.74 (0.64, 0.86)
AMD
Start of follow-up (free of AMD and cataract)
Transition A HR=1.59 (1.38, 1.82)
AMD
Transition C HR=2.76(2.64, 2.89)
Transition B HR=0.96 (0.80, 1.16)
Cataract
D
Start of follow-up (free of AMD and glaucoma)
Transition A HR=1.82 (1.68, 1.96)
Glaucoma
Transition C HR=1.73 (1.62, 1.86)
Transition B HR=1.50 (1.15, 1.96)
AMD
Start of follow-up (free of AMD and glaucoma)
Transition A HR=1.74 (1.63, 1.86)
AMD
Transition C HR=1.80 (1.67, 1.95)
Transition B HR=1.42 (1.06, 1.91)
Glaucoma
E
Start of follow-up (free of cataract and glaucoma)
Transition A HR=1.54 (1.45, 1.64)
Cataract
Transition C HR=1.95 (1.64, 2.31)
Transition B HR=1.18(0.91, 1.54)
Glaucoma
Start of follow-up (free of glaucoma and cataract)
Transition A HR=1.91 (1.63, 2.23)
Glaucoma
Transition C HR=1.54(1.44, 1.64)
Transition B HR=1.05 (0.82, 1.35)
Cataract
F
chr1
1q42.12
chr3
3q26.33
chr5
5q14.3
chr9
9p21.3
chr11
11q13.2
11q14.2
chr12
12q13.2
12q24.11
chr15
15q12
chr16
16q22.1
chr17
17q25.3
0bp
50Mb
100Mb
150Mb
200Mb
250Mb
Length (bp)
AMD_cataract
AMD_glaucoma
cataract_glaucoma
Posterior probability
0.8
0.6
0.4
0.2
0.0
chr9
5Mb
10Mb
20Mb
30Mb
40Mb
Length (bp)

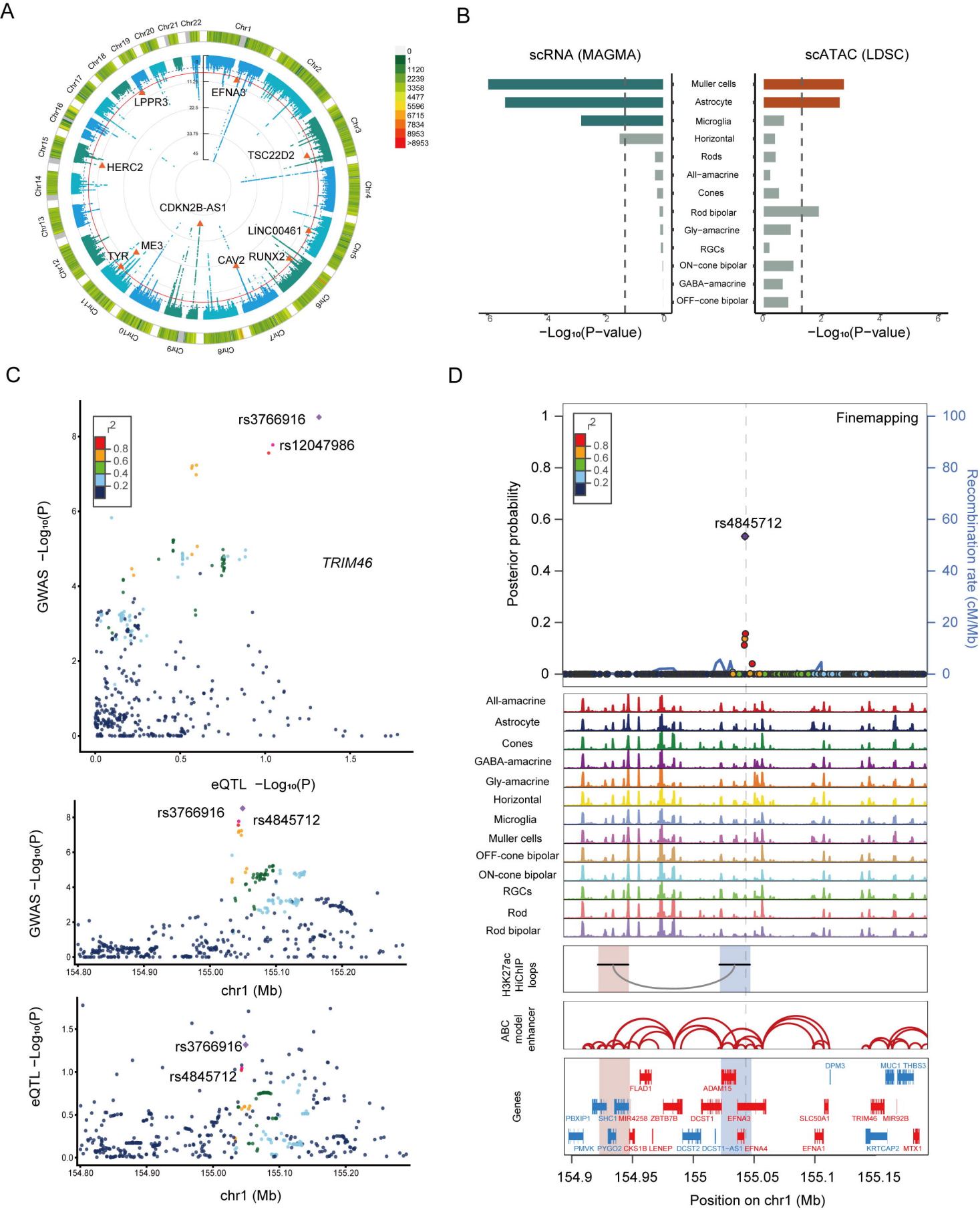
A
Chr1
Chr2
Chr3
Chr4
Chr5
Chr6
Chr7
Chr8
Chr9
Chr10
Chr11
Chr12
Chr13
Chr14
Chr15
Chr16
Chr17
Chr18
Chr19
Chr20
Chr21
Chr22
EFNA3
LPPR3
TSC22D2
HERC2
CDKN2B-AS1
LINC00461
ME3
TYR
CAV2
RUNX2
0
1
1120
2239
3358
4477
5596
6715
7834
8953
>8953
B
scRNA (MAGMA)
scATAC (LDSC)
Muller cells
Astrocyte
Microglia
Horizontal
Rods
All−amacrine
Cones
Rod bipolar
Gly−amacrine
RGCs
ON−cone bipolar
GABA−amacrine
OFF−cone bipolar
−Log10(P−value)
−Log10(P−value)
C
rs3766916
rs12047986
r2
0.8
0.6
0.4
0.2
TRIM46
GWAS −Log10(P)
eQTL −Log10(P)
rs3766916
rs4845712
GWAS −Log10(P)
chr1 (Mb)
rs3766916
rs4845712
eQTL −Log10(P)
chr1 (Mb)
D
Finemapping
r2
0.8
0.6
0.4
0.2
rs4845712
Posterior probability
Recombination rate (cM/Mb)
All-amacrine
Astrocyte
Cones
GABA-amacrine
Gly-amacrine
Horizontal
Microglia
Muller cells
OFF-cone bipolar
ON-cone bipolar
RGCs
Rod
Rod bipolar
H3K27ac HiChIP loops
ABC model enhancer
Genes
DPM3
MUC1
THBS3
FLAD1
ADAM15
PBXIP1
SHC1
MIR4258
ZBTB7B
DCST1
EFNA3
SLC50A1
TRIM46
MIR92B
PMVK
PYGO2
CKS1B
LENEP
DCST2
DCST1-AS1
EFNA4
EFNA1
KRTCAP2
MTX1
Position on chr1 (Mb)

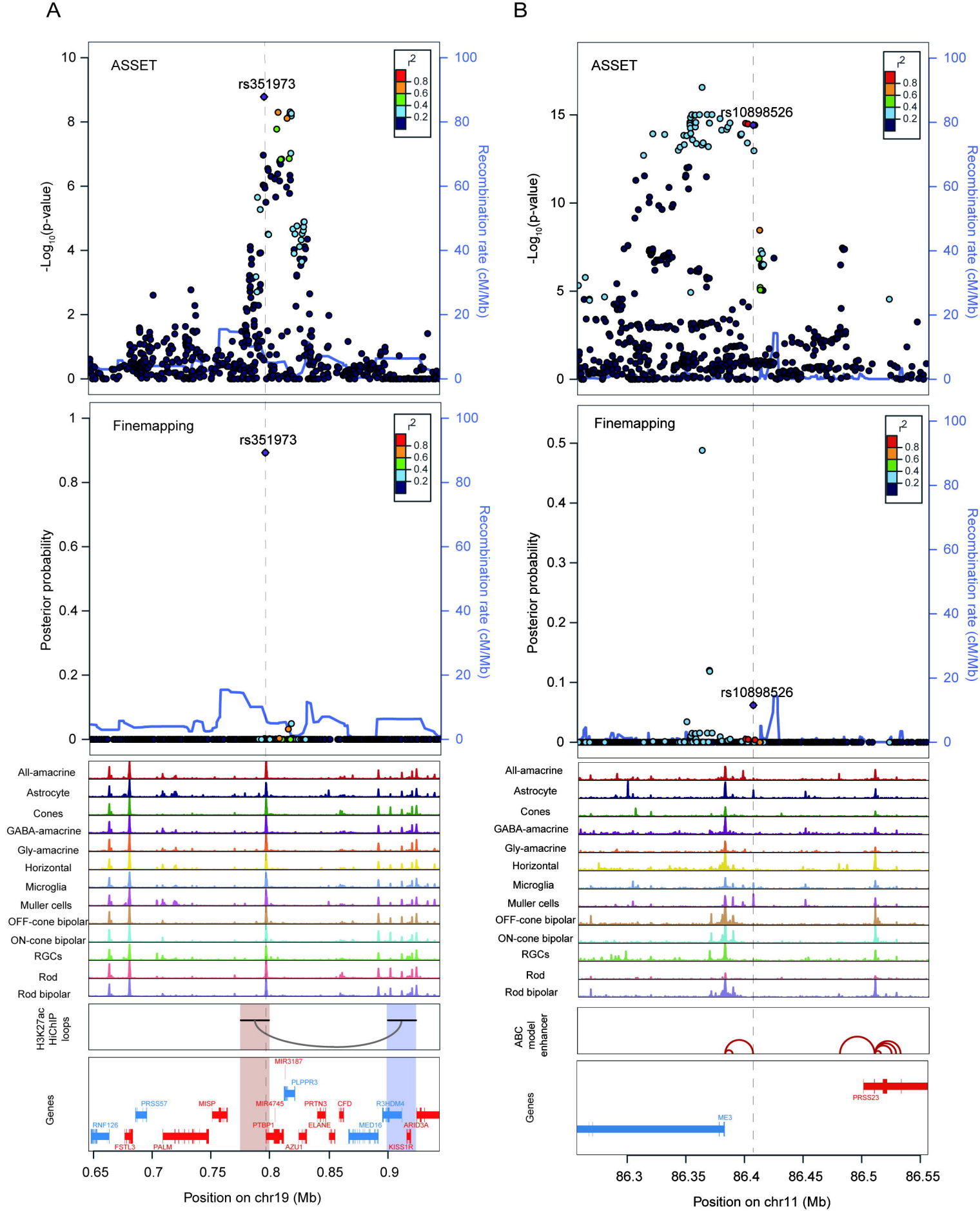
A
B
ASSET
rs351973
rs10898526
Finemapping
-Log10(p-value)
Posterior probability
Recombination rate (cM/Mb)
r2
0.8
0.6
0.4
0.2
All-amacrine
Astrocyte
Cones
GABA-amacrine
Gly-amacrine
Horizontal
Microglia
Muller cells
OFF-cone bipolar
ON-cone bipolar
RGCs
Rod
Rod bipolar
H3K27ac HiChIP loops
ABC model enhancer
Genes
MIR3187
PLPPR3
PRSS57
MISP
MIR4745
PRTN3
CFD
R3HDM4
RNF126
PTBP1
ELANE
MED16
ARID3A
FSTL3
PALM
AZU1
KISS1R
PRSS23
ME3
Position on chr19 (Mb)
Position on chr11 (Mb)

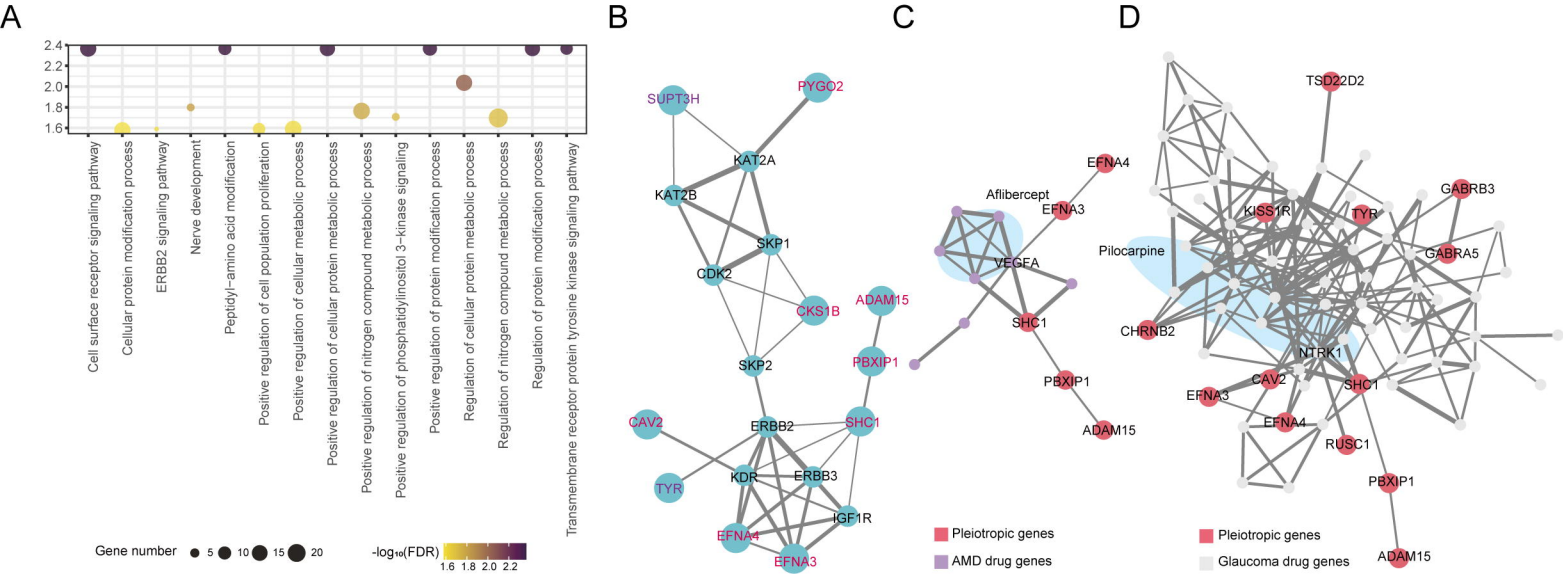
A
2.4
2.2
2.0
1.8
1.6
Cell surface receptor signaling pathway
Cellular protein modification process
ERBB2 signaling pathway
Nerve development
Peptidyl−amino acid modification
Positive regulation of cell population proliferation
Positive regulation of cellular metabolic process
Positive regulation of cellular protein metabolic process
Positive regulation of nitrogen compound metabolic process
Positive regulation of phosphatidylinositol 3−kinase signaling
Positive regulation of protein modification process
Regulation of cellular protein metabolic process
Regulation of nitrogen compound metabolic process
Regulation of protein modification process
Transmembrane receptor protein tyrosine kinase signaling pathway
Gene number
5
10
15
20
-log10(FDR)
1.6
1.8
2.0
2.2
B
SUPT3H
PYGO2
KAT2A
KAT2B
SKP1
CDK2
CKS1B
SKP2
CAV2
ERBB2
SHC1
TYR
KDR
ERBB3
IGF1R
EFNA4
EFNA3
ADAM15
PBXIP1
C
EFNA4
Aflibercept
EFNA3
VEGFA
SHC1
PBXIP1
ADAM15
Pleiotropic genes
AMD drug genes
D
TSD22D2
GABRB3
KISS1R
TYR
Pilocarpine
GABRA5
CHRNB2
NTRK1
CAV2
SHC1
EFNA3
EFNA4
RUSC1
PBXIP1
ADAM15
Pleiotropic genes
Glaucoma drug genes